

In-Flight Estimation of Gyro Noise on the Upper Atmosphere Research Satellite (UARS) and Extreme Ultraviolet Explorer (EUVE) Missions*

M. Lee, P. Crouse, and R. Harman
National Aeronautics and Space Administration (NASA)
Goddard Space Flight Center (GSFC)
Greenbelt, Maryland, USA

T. Leid, W. Davis, and S. Underwood
Computer Sciences Corporation (CSC)
Lanham-Seabrook, Maryland, USA

Abstract

This paper characterizes the low-frequency noise response of the Teledyne dry rotor inertial reference unit (DRIRU) gyroscopes on the Upper Atmosphere Research Satellite (UARS) and the Extreme Ultraviolet Explorer (EUVE). The accuracy of spacecraft attitude estimation algorithms that use gyro data for propagating the spacecraft attitude is sensitive to gyro noise. EUVE gyro data were processed to validate a single-axis gyro noise model, which is used onboard various spacecraft. The paper addresses the potential impact of temperature effects on the gyro noise model and the overall impact on attitude determination accuracy. The power spectral density (PSD) of the gyro noise is estimated from UARS in-flight data by Fast Fourier Transform (FFT). The role of actuator dynamics on the PSD function is also discussed.

Introduction

The algorithms that use gyro data to propagate the spacecraft attitude over a period of time are affected by the estimation of the gyro noise. This paper attempts to characterize that noise by using in-flight data for the Upper Atmosphere Research Satellite (UARS) and the Extreme Ultraviolet Explorer (EUVE). Both UARS and EUVE have Teledyne dry rotor inertial reference unit (DRIRU)-II gyroscopes on board. The description and specifications of this hardware are presented below.

One goal of this paper is to use in-flight data to validate a single-axis gyro model that is commonly used in the Kalman filter attitude estimation process on board various spacecraft (the Gamma Ray Observatory (GRO), EUVE, and UARS, for example) to estimate gyro rate and drift rate noise. Since EUVE has redundant measurements on all three axes, it is proposed that the difference of the two measurements will strip the true rate information and leave the noise. This noise then can be evaluated to determine if the model is accurate. A second goal of this work is to attempt to identify the source of signatures in the gyro data for the UARS spacecraft. The solar array drive is known to cause real spacecraft motion that is reported in the gyro data. It has been suggested that components of the gyro data that appear to be measurement noise may be due to science instrument operation. The power spectral density (PSD) of the gyro noise will be obtained by Fast Fourier Transform (FFT) to evaluate this suggestion. The goal is to be able to reduce the estimate of gyro noise to a value that is only the true noise so that attitude determination accuracy can be improved.

*This work was supported by the National Aeronautics and Space Administration (NASA)/Goddard Space Flight Center (GSFC), Greenbelt, Maryland, under Contract NAS 5-32500.

IRU Description and Specifications

The DRIRU II consists of three gyroscopes, each with a spinning rotor mounted on two gimbals to provide 2 degrees of freedom and rate information along two body axes (two channel output), for a total of six channels of information. Each gyroscope has internal temperature compensation, and the temperature of each is reported in the downlinked telemetry. The gyroscopes are configured to provide dual redundancy along each body axis. When the spacecraft attitude is noninertial, the IRU gimbals are reoriented to maintain a null deflection from an inertial orientation. The current required to produce the magnetic torque to accomplish this reorientation is proportional to the angular rate about the corresponding axis. This torque current is converted to a series of pulses, which are counted and reported as accumulated rotation angles. The IRU itself provides rate information as incremental angles every 64 milliseconds, and a separate electronics unit converts this to accumulated angles reported every 128 milliseconds for the EUVE. In contrast, the UARS IRU reports digital rates every 128 milliseconds and accumulated angles every 1.024 seconds. In our following analysis, the IRU and the electronics unit are considered together as the IRU.

The IRU can operate in two rate ranges. The high-rate mode allows for rates of up to 2.0 degree/second (deg/sec); low-rate mode allows rates of up to 400 arcsec/sec (.11 deg/sec). The digital resolution of the IRU is 0.8 arcsec in high-rate mode and .05 arcsec in low-rate mode. The specified angular rate bias stability (Reference 1) for the DRIRU is on the order of 0.003 arcsec/sec over a period of 6 hours and 0.02 arcsec/sec over a month. The long-term noise characteristics of the DRIRU differ from the short term, so the random walk noise model is appropriate only for relatively short timespans (on the order of at least 6 hours). Only the short-term noise performance is pertinent for the onboard attitude determination processing.

The IRU accumulated rotational angle measurements are reported in the EUVE telemetry as integer counts at 0.128-sec intervals. The Flight Dynamics Facility (FDF) ground system unpacks and converts the counts to engineering units (deg/sec) while also (optionally) correcting the measurements for known misalignments, scale factors, and biases.

Noise Model and Rate Noise

A common model for IRU rate noise (documented in Reference 2 and used in the onboard Kalman filter for attitude determination) uses the sum of two noise processes:

$$r(t) = v(t) + b(t)$$

where $r(t)$ is the rate noise as a function of time, $v(t)$ is a rapidly varying random process that is modeled by a white-noise source, and $b(t)$ is a slowly varying random process that is modeled by a random walk process (see Reference 2), with the rate white noise, $v(t)$, corresponding to the float torque noise and the bias white noise, $u(t)$, corresponding to the float torque derivative noise. We intend $b(t)$ to be the variations of the rate bias. It is the amount of accumulated bias error since the beginning of some timespan. As the initial bias will be calculated and adjusted for in our processing, the value of $b(t)$ can be taken as zero at the start time, t_0 , of the timespan under consideration. The autocorrelation of the white-noise source has the following form:

$$\langle v(t)v(t') \rangle = \sigma_v^2 \delta(t-t')$$

where σ_v^2 has the dimensions of angle squared per time and $\langle \dots \rangle$ is the statistical expectation operator. The random walk process is the integral of another independent white-noise source. Let $u(t)$ be the white noise source that drives the random walk of the rate such that

$$\langle u(t)u(t') \rangle = \sigma_u^2 \delta(t-t')$$

where σ_u^2 has the dimensions of angle squared per time cubed. Then, the random-walk process is then given by

$$b(t) = \int_{t'=t_0}^{t'=t} u(t') dt'$$

$$\langle b(t)b(t') \rangle = \int_{t_1=t_0}^{t_1=t} dt_1 \int_{t_2=t_0}^{t_2=t'} dt_2 \langle u(t_1)u(t_2) \rangle$$

$$\langle b(t)b(t') \rangle = \sigma_u^2 \min((t-t_0), (t'-t_0))$$

where $\min((t-t_0), (t'-t_0))$ is the smaller of $t-t_0$ and $t'-t_0$. For independent random processes, the autocorrelation of the rate noise is given by

$$\langle r(t)r(t') \rangle = \sigma_r^2 \delta(t-t') + \sigma_u^2 \min((t-t_0), (t'-t_0))$$

Observable Consequences of Rate Noise

The rate output of the IRU for each channel has the following form

$$\Omega(t) = \omega(t) + r(t)$$

where $\Omega(t)$ and $\omega(t)$ are the observed and true rates, respectively. The IRU converts this rate to an accumulated angle

$$\Theta(t) = \int \Omega(t) dt = \int \omega(t) dt + \int r(t) dt$$

Let the rate be integrated from time t_0 . Let $q(t)$ be the noise of the integrated rate as a function of time. Then,

$$q(t) = \int_{t'=t_0}^{t'=t} r(t') dt' = \int_{t'=t_0}^{t'=t} v(t') dt' + \int_{t'=t_0}^{t'=t} b(t') dt'$$

Note that because the integral of a white noise source is a random walk, the rate white noise source becomes a random walk process for the accumulated angle. Also, the rate random walk process becomes a double random walk for the accumulated angle. The phrase "random walk" by itself becomes ambiguous. It could mean either the random walk of the rate, which is produced by the u-process, or the random walk of the angle, which is caused by the v-process.

The variance of the noise of the angle accumulated from time t_0 is

$$\begin{aligned} \langle q(t)^2 \rangle &= \int_{t'=t_0}^{t'=t} dt' \int_{t''=t_0}^{t''=t} dt'' (\langle v(t')v(t'') \rangle + \langle b(t')b(t'') \rangle) \\ &= \sigma_v^2 (t-t_0) + \int_{t'=t_0}^{t'=t} dt' \int_{t''=t_0}^{t''=t} dt'' \sigma_u^2 \min(t'-t_0, t''-t_0) \\ &= \sigma_v^2 (t-t_0) + \frac{1}{3} \sigma_u^2 (t-t_0)^3 \end{aligned} \quad (1)$$

The verification of the above equation is the goal of our gyro noise processing. For EUVE, all six gyro channels are reported in the downlinked telemetry. This luxury allows us to observe the gyro noise directly. If timespans of data

are used where the spacecraft is undergoing constant rate motion and if small effects due to the slight differences in alignments of the gyro channels are neglected, then the result of differencing the primary and backup gyro signals for a given axis will be to subtract the true rate information. One is then left with a quantity equal to the difference of the two channels' rate biases and rate noises. If the initial bias of these quantities is removed, a source of pure noise is left that theoretically is described by the above equation, but with the root mean square (RMS) strength of the random walk sources for the gyros given by

$$\sigma_v / (\sqrt{2}) \tag{2}$$

and

$$\sigma_u / (\sqrt{2})$$

An additional quadratic term can be included in Equation (1), $\sigma_b^2 (t - t_0)^2$, which is due to the 1-sigma uncertainty, σ_b , in the initial bias calculation. The bias uncertainty is discussed later in this analysis.

Results from Applying the Noise Model to Observed Data

Both low-rate mode and high-rate mode gyro noise were investigated. To minimize contributions to noise and bias changes due to spacecraft motion and gyro misalignment coupling, only timespans where EUVE was rotating at a constant rate were processed. For the low-rate mode, this implies that EUVE is inertially pointing, while for high-rate, the survey phase data could be used. During the survey phase, EUVE is rotating at a constant rate of 3 revolutions per orbit most of the time. As discussed below, because finding inertial data for this analysis was difficult, eventually timespans when EUVE was in the survey phase were used exclusively.

In Figure 1, the square of the propagated error due to the noise differences from the primary and backup X channels is shown as a function of propagation time in seconds for a span of data on December 11, 1993. At this time, the gyros were in the low-rate mode. Comparison of the shape of the variance plot over time (Figure 1) versus the temperature plot (for the primary X channel, Figure 2) suggests that the gyro parameters might be affected by temperature changes. Further investigation into the data shows that for the data taken on that day, the apparent bias (computed at 5-minute intervals), is roughly linear with respect to the average (over the prime and backup channels) temperature as shown in Figure 3. As the bias is the average difference between two gyro signals for a given axis, both gyros must have constant temperatures to avoid temperature-variation induced effects. From the data processing performed for this analysis, it is unclear whether other gyro parameters, such as the gyro scale factor for conversion of the telemetered counts to engineering units or the random noise strengths, are also functions of temperature. Previous analysis for the Cosmic Background Explorer (COBE), Reference 3, has shown gyro parameter dependence on gyro temperatures, although the gyros flown on COBE were not the DRIRU II. The COBE experience was that a variation in drift rate was seen approximately 320 seconds after a change in gyro base plate temperature. Note that the bias variation, as a function of time, appears correlated to the gyro temperature change, and the propagation error plotted in Figure 1 is the integral with respect to time of the bias. Further analysis is planned to characterize the relationship of the changes in the DRIRU II parameters with temperature variation.

In general, the gyro temperature varied more when EUVE was inertial than when EUVE was in survey mode. Because of the rotation during the survey phase, the gyro temperatures are more likely to remain constant over several hours in time. For this reason, only EUVE survey mode data were used.

Another problem, one that plagued previous attempts (Reference 4) to fit the gyro noise model to on-orbit data, is that the best cubic fit to the data often entails negative coefficients for the fitting polynomial if the bias uncertainty term (the quadratic term) is allowed free rein. Negative values of these coefficients are not physically meaningful in the noise model. To circumvent this problem, the quadratic term that models the contribution of uncertainty in the initial bias to the propagated error is analyzed in detail.

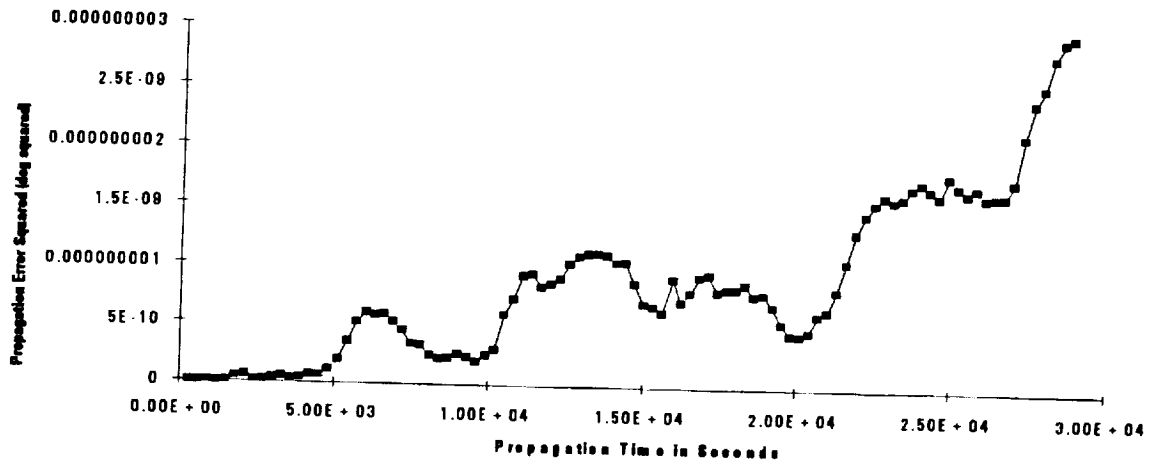


Figure 1. X Propagation Error Squared for December 11, 1993 (Low Rate)

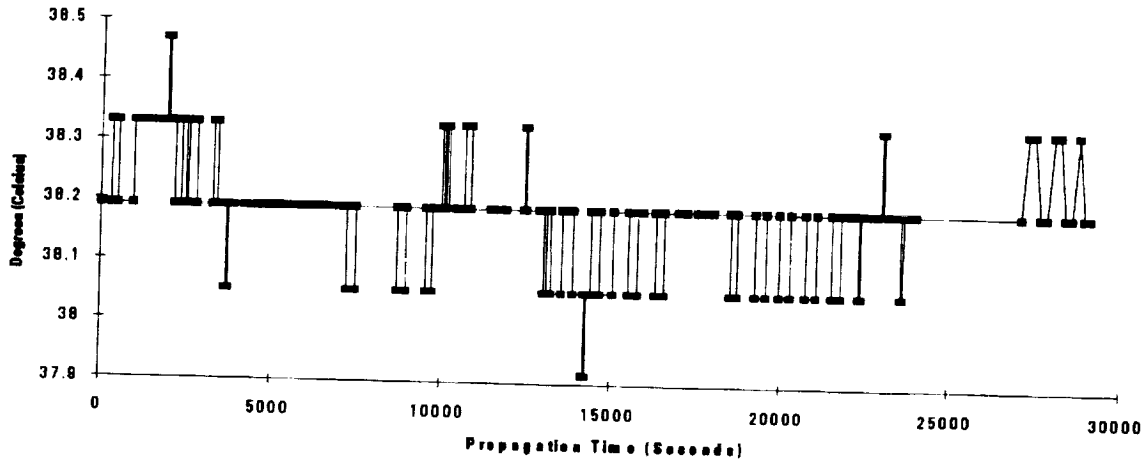


Figure 2. Prime and X and Y Channel Temperature for December 11, 1993

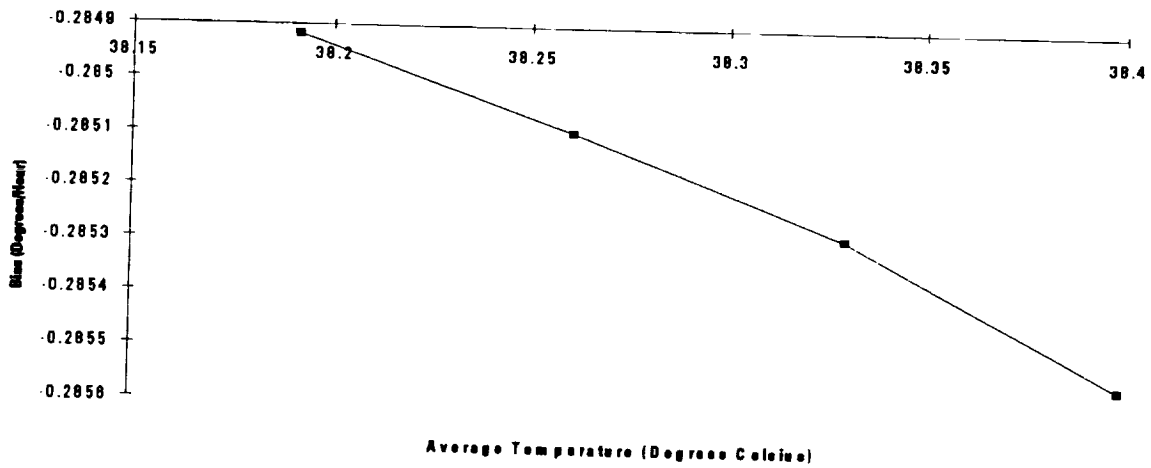


Figure 3. X Channel Bias Versus Average (Prime and Backup) Temperatures

The initial bias used is the average gyro signal over the first 5 minutes of data taken. The one-sigma error in an individual bias computation due to accumulated noise, telemetry quantization, and variation of the bias over the first 5 minutes (using the random walk noise model) can be estimated. This error is dominated by the error caused by the rate white noise, with strength denoted by σ_v . Over a 5-minute interval, the accumulated angle error variance is given by $\sigma_v^2 \cdot 300(\text{sec})$, with the resultant bias variance, σ_b^2 , given by $\sigma_v^2 / 300(\text{sec})$. This results in the final equation for the variance of the noise of the angle accumulated from time t_0 given by

$$\langle q(t)^2 \rangle = \sigma_v^2 \left[(t - t_0) + (t - t_0)^2 / 300(\text{sec}) \right] + \frac{1}{3} \sigma_u^2 (t - t_0)^3 \quad (3)$$

Survey data from September 5 through September 11, 1992, was processed for this analysis. The FDF received slightly over 4 hours of continuous data for each of these days, and all of the available data for these days were used. The average over all of the gyro channels for each of the days processed (seven intervals) of the propagation variance was assumed to be of the form

$$Q(\Delta t)^2 = a_1 (\Delta t + \Delta t^2 / 300 \text{sec}) + a_3 (\Delta t)^3 \quad (4)$$

and a least squares fit to the parameters a_1 and a_3 was performed. The temperature dependence of the white noise strength parameters is neglected. The parameters computed will reflect the RMS of the white noise strength parameters over all the gyro channels. The final procedure is described below:

1. Find timespans of data that are at a nearly constant rate for the entire timespan; for EUVE, we used the playback survey mode data from September 5 through September 11, 1992.
2. Ensure that there are no extreme temperature variations of the gyros. By visual inspection of the data, the temperature varied no more than 1 sensor count (.14 deg Celsius) from its median value for the days chosen (with the exception of infrequent, short-lived peaks of 2 counts, which are possibly noise in the temperature sensor output).
3. Process the primary and backup channel information for each axis, differencing the backup channel from the primary channel to remove the signal and leave only the value of the backup channel's noise subtracted from the primary channel's noise and the difference in the two channels' biases.
4. Compute the initial bias using a 5-minute timespan and compensate for the initial bias throughout the timespan of data used.

The cubic equation describes the model for the variance of the accumulated angle due to gyro noise or equivalently the expected value of the noise-driven propagation error squared. The gyro noise samples are accumulated (or propagated) over time, and a least squares fit to Equation (4) is performed on the average (over all timespans and over all gyro axes) square of the gyro noise propagation error. The white noise strengths σ_v and σ_u indicated by the data taken can then be calculated and compared to expected values.

A total of 21 sample points of the propagation variance (3 axes and 7 days) is available for propagation times over 4 hours. The 4-hour length is constrained by the length of the data routinely provided the FDF on a given day. The 21 points give an average propagation error (squared) that can be fit to Equation (2) with results depicted in Figure 4. Data points are indicated by the squares; the fitting curve is the dark line.

The 1-sigma white noise strengths for an individual channel that corresponds to the cubic fit shown above are

$$\sigma_v = 0.12 \text{ arcsec} / \text{sec}^{1/2} \quad (5)$$

and

$$\sigma_u = 5.21 \times 10^{-5} \text{ arcsec} / \text{sec}^{3/2}$$

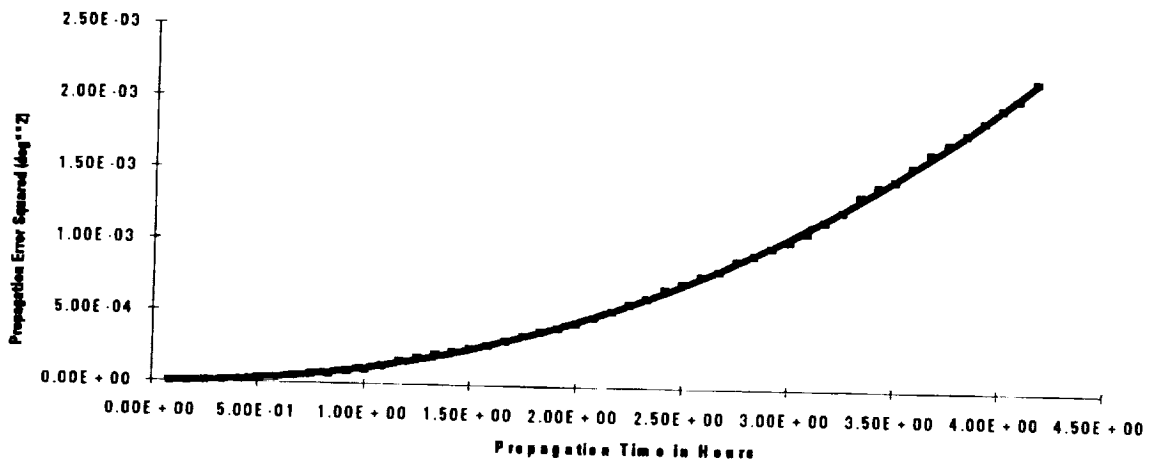


Figure 4. Average Variance Over All Channels (High Rate)

Typical values used for the DRIRU II in low-rate mode, (for GRO and EUVE, for example), are

$$\sigma_v = 0.042 \text{ arcsec}/\text{sec}^{1/2}$$

and

$$\sigma_u = 4.44 \times 10^{-5} \text{ arcsec}/\text{sec}^{3/2} \quad (6)$$

Our values are for the DRIRU II in high-rate mode, so no direct comparison can be made except that the computed values are higher and on the same order of magnitude. This comparison to the onboard numbers, which are based on ground analysis for the low-rate mode, is made mainly to verify our results. Since our results are for the DRIRU II in the high-rate mode and the EUVE and GRO values are for the low-rate mode, attempting to draw any further conclusions about the accuracy of the onboard numbers would be specious because the parameters could differ depending on the rate mode. Based on these data, the onboard white noise strengths used by the EUVE onboard Kalman filter when the gyros were in the high-rate mode should have been increased from the expected values of gyros in the low-rate mode.

Discussion of Results

The first goal, to validate the noise model using on-orbit data, can be considered accomplished, although only for the DRIRU II in high-rate mode and for EUVE in survey mode so that temperature effects are reduced. The cubic fit to the average covariance of the propagation error due to noise is accurate enough from a practical sense for onboard processing. Furthermore, early in the mission, when EUVE was using the gyros in the high-rate mode (necessary for the survey phase), the gyro noise parameters used by the onboard Kalman filter were for the low-rate mode. Based on the white noise strengths computed for the high-rate mode, this could cause a decrease in the accuracy of the onboard attitude determination algorithm, and was, in fact, seen (Reference 5). Based on recommendations from the FDF, the low-rate mode was used when possible for EUVE to improve the onboard attitude determination. Another solution would have been to tailor the noise parameters to the high-rate case when the gyros were in high-rate mode.

However, the difficulties due to changing gyro temperatures do cause concern. As discovered during our analysis, the gyro parameters appear to be temperature dependent to a degree that might impact the usefulness of the noise model. Further analysis is necessary, using low-rate data when EUVE is inertially fixed, to quantify the impact of the temperature dependence on the noise model accuracy for the low-rate scenario.

Potential topics for further analyses are as follows:

1. Investigate the temperature effects on the gyro parameters
2. Continue analysis of the low-rate mode to determine the impact of the temperature dependence on the applicability of the noise model
3. Process further data and compute the statistical confidences of the results

Power Spectral Analysis

The aim in using the power spectra of the gyro noise is (1) to identify the signals associated with the operation of the solar array and science instruments and (2) to obtain a baseline signature of the gyro noise as a diagnostic aid. It has been the experience of the FDF (GSFC) that gyro failure can be predicated from an increase in gyro noise. Signal detection is best accomplished by using frequency analysis rather than time domain analysis. Power spectra method has an extensive literature base (References 6 and 7), but we follow basically the development in Reference 7.

For a continuous function, $h(t)$, there exists a Fast Fourier Transform (FFT) $H(f)$ if the integral over all times, t , of the absolute value of the function (time series) is bounded or if the function $h(t)$ is monotonically decreasing function of t or if the $h(t)$ can be represented by a curve of finite height in any finite time. Since the gyro data are sampled discretely, rather than continuously, the FFT is correctly represented only with the range of the Nyquist frequency, f_c to f_c , or that the transform is band limited. The Nyquist frequency is defined as $(1/2T)$, where T is the sampling interval.

If the function $h(t)$ is continuous, then a sample of $h(t)$ at times separated by T can be represented as

$$\sum_{n=-\infty}^{n=\infty} h(t) \delta(t - nT) \quad (7)$$

and is an infinite sequence of equidistant impulses (from the delta function) each of whose amplitude is given by the value of $h(t)$ at the time of occurrence. A truncation function, $x(t)$, must be used since the sample signal is of finite duration. The truncation (or window) function is defined below for a given duration T_0 .

$$\begin{aligned} x(t) &= 1 & -T/2 < t < T_0 - T/2 \\ &= 0 & \text{otherwise} \end{aligned} \quad (8)$$

Thus, the expression $h_s(t)$

$$h_s(t) = \sum_{n=-\infty}^{n=\infty} h(t) \delta(t - nT) x(t) \quad (9)$$

represents $N = T_0/T$ sample points of the function $h(t)$. The truncation of the time series introduces rippling in the FFT. The discrete FFT of truncated sample wave form is given by

$$H(n/NT) = \sum_{n=-N}^{N-1} \sum_{m=-\infty}^{\infty} h(t) \delta(t - nT) x(t) e^{i2\pi m n / N} \quad (10)$$

We use the FFT algorithm, popularized by Cooley and Tukey, to compute the FFT of the truncated sampled gyro signal. To obtain the power spectral density function of $h_s(t)$, suppose that the number of observations $N = 2q + 1$ is odd. If we use a Fourier series to model the time series, such as,

$$z(t) = \alpha_o + \sum_{i=1}^q \{\alpha_i \cos(2\pi f_i t) + \beta_i \sin(2\pi f_i t)\} + \varepsilon(t) \quad (11)$$

where $f_i (= i/T)$ is the i^{th} harmonic of the fundamental frequency $(1/T)$ and $\varepsilon(t)$ is the random noise with zero mean and constant variance σ^2 . The terms in the curly bracket represent the signals produced by the solar array movement and the operation of the science instruments. A least squares estimate of the coefficients α_o , α_i , and β_i yields for $i = 1$ through q

$$\begin{aligned} a_o &= \text{gyro bias } \langle z(T) \rangle \\ a_i &= (2/N) \sum_{m=1}^N z(mt) \cos(2\pi f_i t) \\ b_i &= (2/N) \sum_{m=1}^N z(mt) \sin(2\pi f_i t) \end{aligned} \quad (12)$$

The spectral power or amplitude in the i^{th} harmonic is

$$P(f_i) = (N/2)(a_i^2 + b_i^2) \quad i = 1, 2, 3, \dots, q \quad (13)$$

and result for even N is similar except that the b_i are zero. The FFT of the gyro rates would yield the harmonic content of the gyro rates, i.e., the a_i and, subsequently, the power spectral density. The expectation value of the variance of the time series is related to the PSD in a simple way.

$$\sum_{i=1}^N (z(t) - \langle z(t) \rangle)^2 = \sum_{i=1}^q P(f_i) \quad (14)$$

If the times series consisted only of white noise, then the amplitude of $P(f)$ would be equal to

$$P(f_i) = 2\sigma^2 \quad (15)$$

and its amplitude would be independent of frequency. White noises ordinarily defined as noise that possess a flat power density spectrum for all frequencies. Evidently, if the PSD has a constant value for all frequencies, the total power represented by the noise would be infinite. In practice, we defined white noise as a flat power spectral density over the frequency range of interest. However, any harmonic content in the times series would add to the value of variance at those harmonic frequencies.

$$P(f_i) = 2\sigma^2 + N(a_i^2 + b_i^2)/2 \quad (16)$$

In practice, it is not very probable that the frequency of the unknown sinusoidal component would match any of the calculated FFT frequencies. More likely, the variance would be spread among several frequencies and resemble a peak with finite width more than a delta function spike.

The PSD is related to the autocorrelation $R_x(t)$ by

$$PSD = \int_{-\infty}^{\infty} R_x(t) e^{-2\pi f t} dt \quad (17)$$

We assume the autocorrelation to be described by

$$\langle v(t)v(t') \rangle = \sigma_v^2 \delta(t-t') \quad (18)$$

and perform the integration to obtain

$$PSD = \sigma_v^2 \quad (19)$$

where the units of σ_v^2 are $\text{angle}^2/\text{time}$ ($\text{arcsec}^2/\text{sec}$). The PSD will have the units of the quantity being analyzed (rad/sec) squared per freq (sec^{-1}). So, our units should be $\text{rad}^2/\text{sec}^2$. However, we are performing the discrete Fourier Transform. The relation between the discrete Fourier transform (H_n) of a set of numbers and their continuous Fourier Transform ($H(f_n)$) when they are viewed as samples of a continuous function sampled at an interval dt can be rewritten as $H(f_n) \approx dt \cdot H_n$. As we are computing the discrete Fourier Transform of the rates and using the square of the magnitudes to represent the PSD, we need to multiply by dt^2 squared to get to an approximation to the continuous PSD, which is related to the continuous autocorrelation (with the delta function) as above.

For low rates, the $0.042 \text{ arcsec}/\text{sec}^{1/2}$ value for the white noise and the equation

$$P(f) = 2\sigma^2 \quad (20)$$

gives a value for our discrete PSD of

$$\begin{aligned} PSD &= 2 \cdot \sigma_v^2 / (.128 \text{ sec})^2 \\ &= 2 \cdot (57.296)^{-2} \cdot 3600^{-2} \cdot 0.042^2 / (0.128)^2 \\ &\approx 5 \cdot 10^{-12} \end{aligned} \quad (21)$$

Two criteria are used to identify significant peaks in the power spectral density. First, only peaks that have amplitude that are at least an order of magnitude larger than the background level are considered. This criterion establishes the signal peak as statistically significant. Secondly, signal peaks that have finite bandwidths are indicative of complex physical processes.

The two main practical limitations for applying the power spectra method are as follows: (1) the length of the times series should not be a multiple of the frequency of interest and (2) the frequency of interest must be below half of the sampling frequency. However, in most cases, one does not know the frequency of interest. The most reasonable way to analyze the power spectra is to obtain spectra for different sample lengths. In this way, the occurrence of false periodicities are minimized.

Power Spectra of UARS Gyroscopic Rates

Data from UARS were used for two basic reasons: (1) the solar array motion was known to induce motion in the spacecraft and (2) some of the scientific instruments were suspected of causing motion in the spacecraft. A search was made of the archival data for timespans in which investigators could isolate noise associated with the quiescent spacecraft from that of the operation of the solar arrays, the science instruments, and nominal operations. For the quiescent period, June 4, 1992, was selected since the science instruments were turned off, and the solar array was parked. On August 8, 1993, there was an extended period when only the solar array was in operation. Three days later, on August 11, at 17:50 Greenwich mean time (GMT), the UARS science instruments were turned on. February 6, 1994, was selected to represent nominal operations.

On board the UARS spacecraft, the gyroscopes' digital rates are sampled every 0.128 sec, which is subsequently sent to the FDF for ground processing. On the ground, the digital rates are converted to gyro rates in units of

rad/sec. These data are ordinarily used to determine the spacecraft's attitude. We applied the FFT to computed gyro rates samples that were of different lengths (15 and 30 min) and different sampling times (1.152 and .128 sec, respectively). The units of the PSD are $\text{rad}^2/\text{sec}^2$.

In Figures 5, 6, and 7, we have the power spectra density function from the quiescent period. The spectra indicates that the noise level of the PSD is about $10^{-12} \text{ rad}^2/\text{sec}^2$. This implies a white noise level corresponds to a digital rate of about 0.2 arcsec/sec. On the X and Z-axis, there are four peaks that are in common to both plots, namely, .24, .97, 1.95, and 2.93 Hertz (Hz). The major difference between these axes is that the peak at .24 Hz on the X-axis is 10 times larger than one on the Z-axis. The Y-axis, which is the pitch axis, is the axis about which UARS rotates once an orbit (1 rpo) and its power spectra does not have a well-defined peak at 0.24 HZ. The pitch axis does, however, have several frequencies of interest. The frequencies are as follows: 0.479 , 0.956 , 1.43, 1.95, 2.44, 2.93., 3.43 Hz.

Data from August 8, 1993, in which only the solar array is operating, shown in Figures 8, 9 , and 10, indicates a large increase in the amplitude on all three axes of at least three orders of magnitude at .24 and .956 Hz. In addition, there is a small peak at 2.15 Hz in the power spectra of the X and Z axis. The pitch axis does not contain this frequency.

Data from August 11, 1993, in which all the science instruments are turned on, does not indicate any new frequencies with a finite width. Likewise, the data from February 6, 1994, does not indicate any significant new frequency information other than a slight increase in the noise level. Figures 11 and 12 are representative samples of the data from the period when the science instruments were turned on and off from nominal operations.

Discussion of Results

The immediate goal of the power spectra analysis, which was to determine whether the method can be used to identify spacecraft motion due to the solar array and science instrument, has been obtained. The signature of the solar array consists of large amplitude noise at 0.24 and 0.967 Hz. Additionally, there is a small peak at 2.15 Hz. There does not seem to be a noise signature associated with the operation of the science instruments.

However, further analysis is needed to explain the presence of a large number of peaks with very narrow frequency bandwidth. The occurrence of these frequencies may be related to bandwidth. It is well known that high-frequency resolution (small bandwidth) leads to large variances of the estimate of power spectra while low-resolution (wide bandwidth) produces a stable estimate (Reference 7). On the other hand, presence of these frequencies may be related to how we compute the gyro rates. The basic time step in both these cases is .128 sec. Finally, the sharp peaks may indicate aliasing or over sampling. The presence of increased noise levels near the Nyquist frequency is the standard indicator of aliasing.

A comparison between the UARS and EUVE power spectras was performed to determine if EUVE gyros had a similar signature to UARS. The calculation of EUVE gyro rates is completely different from that of UARS. The data in Figure 13 indicate well-defined signal peaks at 0.976, 1.953, and 2.93 Hz. The EUVE power spectra in Figure 13 represents FFT of 8,192 points from a time series of 16,384 points. Since the Telemetry Processors (TPs) for EUVE and UARS are so different, but mathematically equivalent, the weight of evidence indicates that the abovementioned peaks may be characteristic of the Teledyne DRIRU II gyroscopes and/or multission spacecraft.

The presence of similar peaks in both power spectral densities rules out computational error in the way rates are computed but does not rule out aliasing. The FFT computer program does not calculate FFT above the Nyquist frequency of the time series, but the time series has not been filtered to remove frequencies above the Nyquist frequency. Note that every point in the time series contributes, in principle, to the amplitude of every harmonic. Further work needs to be done to construct a time series filter that would provide a definitive answer about the significance of the narrow peaks.

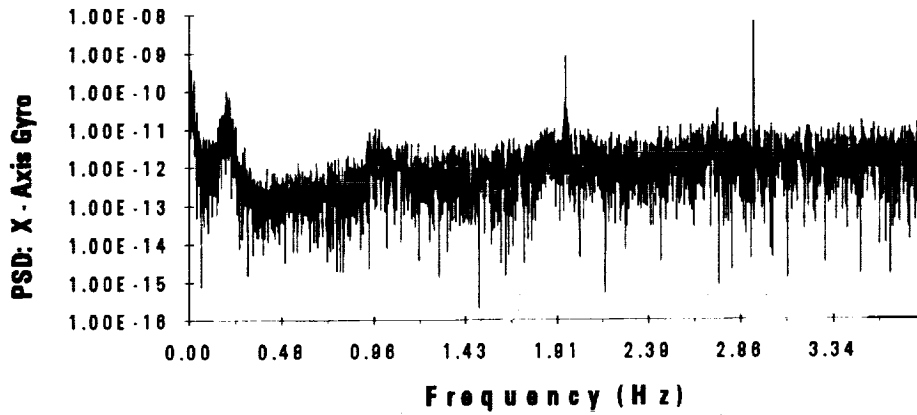


Figure 5. Power Spectra of the X Axis: 920604: (Sample = .128 sec)(N = 8192)

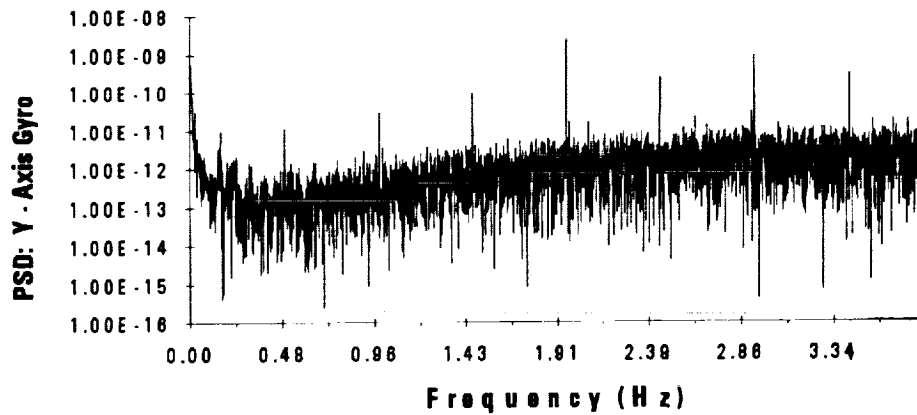


Figure 6. Power Spectra Y Axis: 920604 (Sample time = .128 sec)(N = 8192)

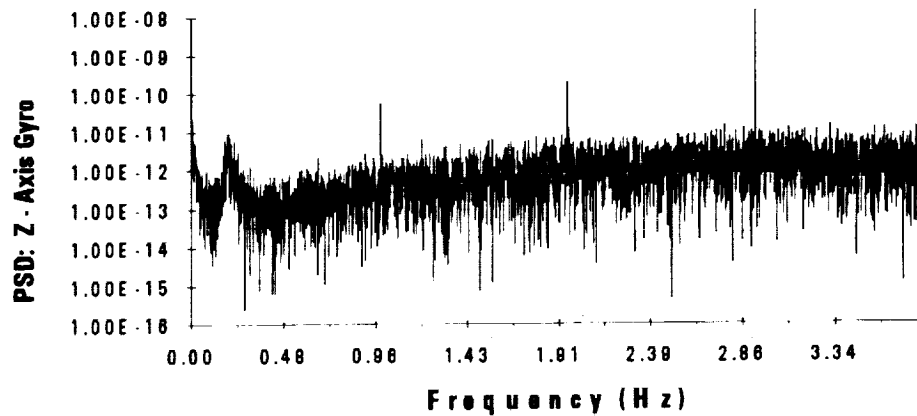


Figure 7. Power Spectra Z Axis: 920604 (Sample time = .128 sec)(N = 8192)

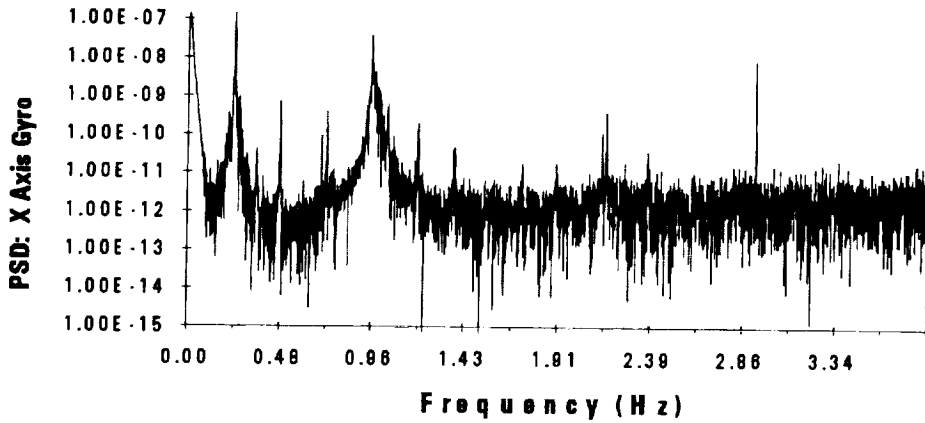


Figure 8. Power Spectra X-axis: 930808 (Sample time = .128 sec) (N = 8192)

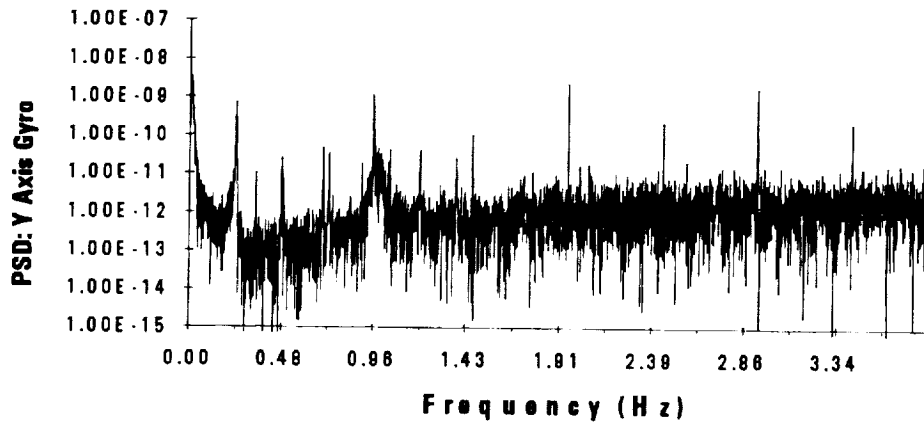


Figure 9. Power Spectra Y-axis: 930808 (Sample time = .128 sec) (N=8192)

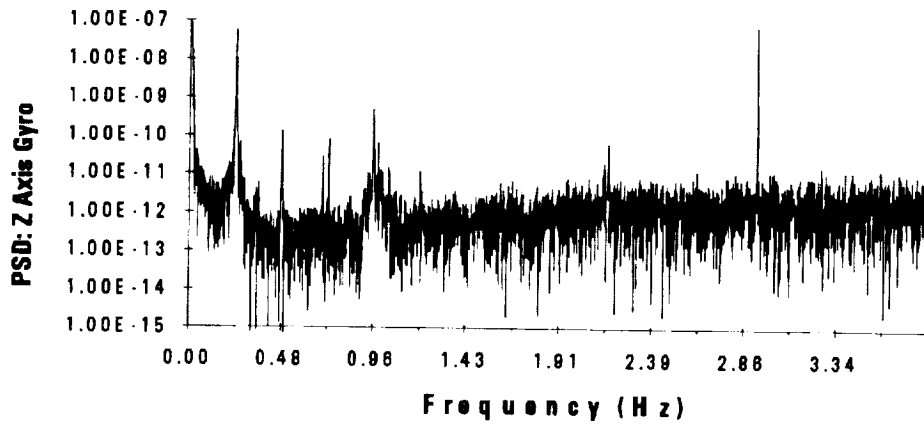


Figure 10. Power Spectra Z-axis: 930808 (Sample time = .128) (N = 8192)

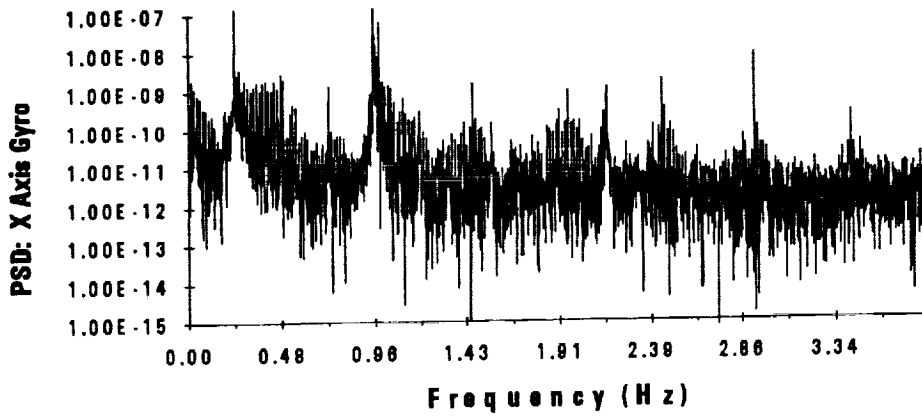


Figure 11. Power Spectra X-axis: 930811 (Sample time = .128 sec) (N = 8192)

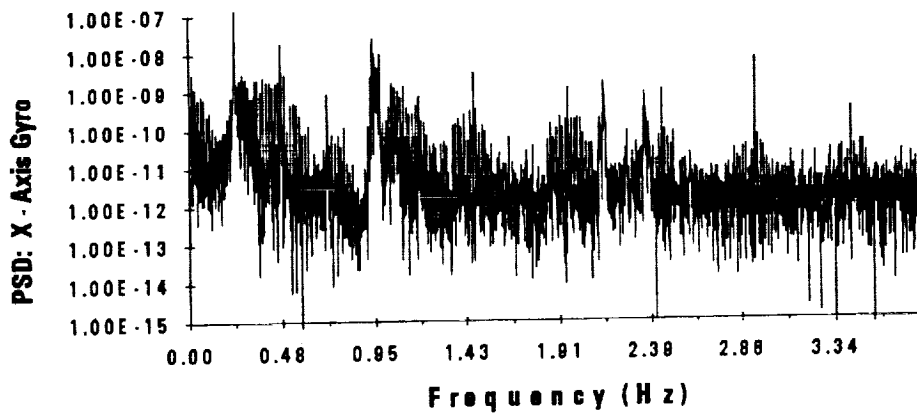


Figure 12. Power Spectra X-axis: 940206 (Sample time = .128 sec) (N = 8192)

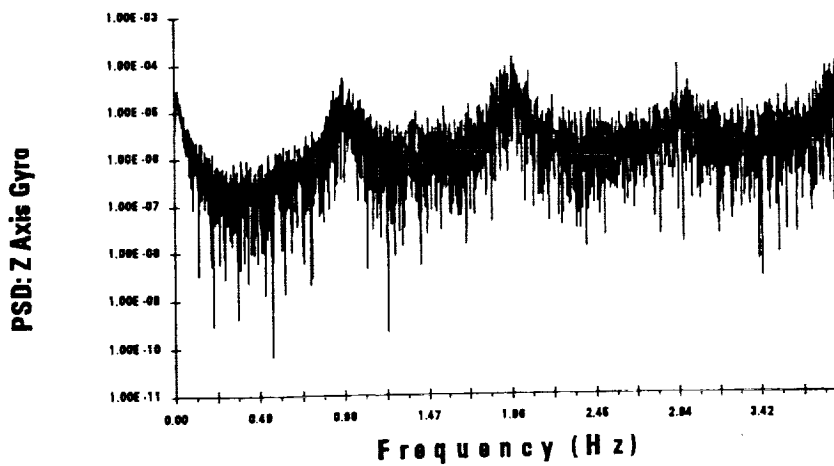


Figure 13. EUVE Coefficients for Z Channel (7/2/92) (N = 16384)

References

1. Teledyne Systems Company, Equipment Specification for High Performance Dry Gyro Inertial Reference Unit (DRIRU II), November 9, 1979
2. R. L. Farrenkopf, "Generalized Results for Precision Attitude Reference Systems Using Gyros," AIAA Mechanics and Control of Flight Conference, Anaheim, CA, August 5-9, 1974, AIAA Paper No. 74-903
3. V. K. Kumar, E. L. Wright, and F. S. Patt, "COBE Ground Segment Attitude Determination," Proceedings of Flight Mechanics and Estimation Theory Symposium, May 21-23, 1991
4. T. Z. Willard, O. H. Filla, D. Chu, and J. Deutschmann, "In-Flight Estimation of Gyro Noise," Proceedings of Flight Mechanics and Estimation Theory Symposium, May 22-24, 1990
5. M. Lee, Memorandum from 553.1/Attitude Section (the Flight Dynamics Facility) to 513/Project Operations Branch/K. Hartnett, January 4, 1993
6. R. B. Blackman and J. W. Turkey, Dover Publications, The Measurement of Power Spectra, Inc., New York, 1959
7. E. O. Brigham, The Fast Fourier Transform and its Applications, Prentice Hall, Englewood Cliffs, New Jersey, 1988

